[CANCER RESEARCH 64, 9185–9192, December 15, 2004]

HOXB13 Induces Growth Suppression of Prostate Cancer Cells as a Repressor of Hormone-Activated Androgen Receptor Signaling

Chaeyong Jung,[1] Ran-Sook Kim,[1] Hong-Ji Zhang,[1] Sang-Jin Lee,[1] and Meei-Huey Jeng[2,3]

Departments of [1]Urology, [2]Medicine, and [3]Microbiology and Immunology, Walther Oncology Center, Indiana University, Indianapolis, Indiana

ABSTRACT

Androgen receptor (AR) signals play a decisive role in regulating the growth and differentiation of both normal and cancerous prostate cells by triggering the regulation of target genes, in a process in which AR cofactors have critical functions. Because of the highly prostate-specific expression pattern of HOXB13, we studied the role of this homeodomain protein in prostate cells. Expression of HOXB13 was limited to AR-expressing prostate cells. Reporter transcription assay demonstrated that HOXB13 significantly suppressed hormone-mediated AR activity in a dose-responsive manner, and suppression was specific to AR with which HOXB13 physically interacts. Overexpression of HOXB13 further down-regulated the androgen-stimulated expression of prostate-specific antigen, and suppression of endogenous HOXB13 stimulated transactivation of AR. Functionally, HOXB13 suppressed growth of LNCaP prostate cancer cells, which could be counteracted by additional hormone-activated AR. On the other hand, the growth-suppressive function of HOXB13 in AR-negative CV-1 cells was not affected by AR. These results suggest that HOXB13 functions as an AR repressor to modulate the complex AR signaling and subsequent growth regulation of prostate cancer cells. In addition to the loss of HOXB13 expression, maintaining AR may be an important step for prostate cancer cells to tolerate the suppressor function of HOXB13. Altogether, our data present a novel mechanism for the HOXB13-mediated repression of AR signaling, which can be interpreted to a growth-suppressive event.

INTRODUCTION

Prostate cancer is the most commonly diagnosed malignancy in men and poses a significant medical problem in the United States. Currently, androgen ablation (chemical or surgical) is the most effective therapy available for advanced prostate cancer, although androgen-independent cancers eventually develop and claim the life of patients. Understanding the complex regulation of androgen signaling is necessary to elucidate the androgen-independent growth of this advanced disease. Androgen receptor (AR) has a key regulatory function in the growth and differentiation of normal and cancerous prostate epithelial cells, triggering the regulation of target genes such as *jun, fos, myc, cdks*, *fibroblast growth factor*, and others. These AR-responsive genes are positively or negatively regulated by recruiting many cofactors into the hormone-receptor complex. Despite the fact that more than 100 steroid receptor cofactors are known, their mechanistic and functional association is not well understood. Only very limited information is available about the negative regulation of hormone-activated AR function.

AR transactivation is initiated upon binding to androgen. Then AR translocates into the nucleus and binds as a homodimer to the cognate DNA response elements on the promoter, where it further interacts with other transcriptional factors and activates downstream gene transcription such as prostate-specific antigen, kallikreins, and calreticulin. AR has distinct functional domains: a highly conserved DNA-binding domain comprising two zinc finger motifs, a COOH-terminal ligand-binding domain, and a poorly conserved NH_2-terminal domain containing one or more transcriptional activation domains. Several cofactors associated with AR have been identified, such as SRC1, AIB1, TIF2, Smad3, BRCA1, CBP, ARAs, and NCoR (reviewed in ref. 1). All of these coregulators can interact with either the COOH- and/or NH_2-terminal domains of AR and regulate AR transactivation. For example, the p160 coactivators SRC1, TIF2, and AIB1 play a central role in mediating transcriptional activation, binding directly to the COOH-terminal activation function domain-2 of nuclear receptors in a ligand-dependent manner. Furthermore, the COOH-terminal region of p160 can also interact with the NH_2-terminal activation function domain-1 domain of some nuclear receptors (2–4). On the other hand, NCoR, an AR corepressor, interacts directly with the AR ligand-binding domain and represses hormone-stimulated AR transcriptional activity (5). These coactivators and corepressors seem to act as accelerators and/or brakes that modulate the transcriptional regulation of hormone-responsive target gene expression, further regulating cell growth. Thus, the discovery of new coactivators and corepressors will expand our knowledge of the mechanisms of steroid receptor action.

Hox homeobox genes encode a set of transcription factors that regulate axial regional specification during embryonic development and are expressed with temporal and spatial colineality. Therefore, *Hox* genes are expressed in a tissue-specific and frequently stage-related fashion. The mammalian *Hox* genes are clustered in four unlinked complexes in the genome (*a b*, *c*, and *d*). Each complex spans approximately 200 kb and contains 9 to 11 genes, composing 39 paralogs (reviewed in 6). The *Hox-13* paralog is important to the development of the prostate. All *Hox-13* genes except *Hoxc13* are expressed in the prostate during embryonic development (7). However, *Hoxa13* and *Hoxd13* are no longer expressed after the embryonic stage (8, 9). *Hoxd13*- and/or *Hoxa13*-deficient mice showed morphologic abnormalities in male accessory sex organs, including the seminal vesicle and prostate (8, 10, 11). *Hoxb13*, the last identified vertebrate *Hox* gene, has been shown to be exclusively expressed in the caudal extent of the spinal cord, tail bud, and urogenital sinus in an androgen-independent manner (12, 13). Mice homozygous for Hoxb13 loss-of-function mutations showed overgrowth in all major structures derived from the tail bud (14) and malformation of ducts of the ventral prostate, including complete loss of secretory proteins (15). Recently, we demonstrated that HOXB13 suppresses the growth of AR-negative PC3 prostate cancer cells by the down-regulation of T-cell factor 4 (TCF-4) expression (16). In this study, we investigated the role of HOXB13 in AR-expressing prostate cancer cells, which may provide new insight into complex AR-signaling pathway mechanisms and a better understanding of its role in prostate carcinogenesis and the progression to androgen-independent prostate cancer.

MATERIALS AND METHODS

Plasmids and Reagents. pFLAG-HOXB13, pIRES-HOXB13, and Ad-GFP-HOXB13 were described previously (16). pGL-AREc-luc was also de-

Received 4/14/04; revised 9/28/04; accepted 10/11/04.

Grant support: Indiana University Biomedical Research Fund grant 22-88-430 and Wendy Will Case Cancer Fund.

The costs of publication of this article were defrayed in part by the payment of page charges. This article must therefore be hereby marked *advertisement* in accordance with 18 U.S.C. Section 1734 solely to indicate this fact.

Requests for reprints: Chaeyong Jung, Department of Urology Indiana University, 1001 10th Street, OPW320, Indianapolis, IN 46202. Phone: 317-278-7617; Fax: 317-278-3432; E-mail: chjung@iupui.edu.

scribed previously (17). Androgen response element core is known as the distal enhancer region of the prostate-specific antigen promoter (18). pGL-ARE4-luc contains a synthetic TATA and four tandem copies of androgen response elements from the murine mammary tumor virus promoter in the context of the pGL3 backbone (Promega, Madison, WI). Estrogen response element–regulated luciferase vector, ERE2-Luc, was provided by Dr. Deborah Lannigan (University of Virginia Health System, Charlottsville, VA). Vectors encoding AIB1 and TIF2 were constructed in pAd1020SfidA (OD260, Inc.) under the control of cytomegalovirus (CMV) promoter. A human AR expression vector, pARO, was a gift from Dr. Jan Trapman (Erasmus University, Rotterdam, The Netherlands). pCMV-βgal was from Promega. Monoclonal antibodies to AR (generated against amino acids 299–315 of AR) and β-actin were from Santa Cruz Biotechnology (Santa Cruz, CA). For coimmunoprecipitation, polyclonal anti-AR antibodies (PG21, Upstate Biotechnology, Lake Placid, NY) were used. Monoclonal anti–prostate specific antigen antibodies were from Dako Cytomation (Carpinteria, CA). Anti-FLAG M5 and anti-c-myc antibodies were from Sigma (St. Louis, MO) and BD Biosciences (San Jose, CA), respectively. Synthetic testosterone, R1881, was from NEN Life Science (Boston, MA) and used at a final concentration of 10 nmol/L.

Cell Culture. Human prostate cell lines, including P69, LNCaP, C4–2, CWR22RV, PC3 and DU145, and LoVo colon cancer cells, were routinely cultured in RPMI (Invitrogen, Carlsbad, CA) supplemented with 5% fetal bovine serum (FBS) at 37°C in an atmosphere containing 5% CO_2 as described previously (19). MDA PCa 2b prostate cancer cells were grown in BRFF-HPC1 medium (Athena Environmental Sciences, Inc., Baltimore, MD) with 20% FBS. CV-1 monkey kidney cells, MCF7A breast cancer cells, and HEK 293 human embryonic renal cells were maintained in Dulbecco's modified Eagle's medium containing 10% FBS. All cultures were fed with fresh medium every 3 to 4 days.

Real-Time Reverse Transcription-Polymerase Chain Reaction. Total RNA from normal human tissues was purchased from Clontech Laboratories (Palo Alto, CA). These RNA were quality-controlled and assured by the company. RNA from prostate, colon, and rectum was obtained from two other different sources to reduce sampling errors. RNA extraction from selected cultured cells and patient samples was performed as described previously (20). Total RNA from PrEc, Pz-HPV7, LAPC-4, and MDA PCa 2a and 2b was generously provided by Dr. Jer-Tsong Hsieh (University of Texas Southwestern Medical Center, Dallas, TX). LNCaP RNA was used for standardizing the expression levels of HOXB13 and glyceraldehyde-3-phosphate dehydrogenase (GAPDH), an internal control. Fifty ng of total RNA from each sample were used to detect real-time reverse transcription-PCR products using Taqman probes and an ABI PRISM 7700 sequence detection system (PE Applied Biosystems, Foster City, CA). PCR cycling conditions were performed for all of the samples as follows: 30 minutes at 48°C for reverse transcription; 10 minutes at 95°C for AmpliTaq Gold activation; and 40 cycles for the melting (95°C, 15 seconds) and annealing/extension (60°C, 1 minute) steps. HOXB13 and GAPDH primers and probes for real-time reverse transcription-PCR were designed using the PRIMER Express program (PE Applied Biosystems). The sequences of the HOXB13 primers and probe are as follows: forward, 5′-ccgggaacctaccacgctat-3′; reverse, 5′-ttctccaggagcacccagagt-3′; probe, 5′-FAM-cagttacctggacgtgtctgtggtgca-TAMRA-3′. The sequences of the AR primers and probe are as follows: forward, 5′-aaggctatgaatgtcagccca-3′; reverse, 5′-cayygaggctagagagcaaggc-3′; probe, 5′-FAM-tgtgtgctggacacgacaacaacc-TAMRA-3′. The sequences of GAPDH primers and probe are as follows: forward, 5′-gaaggtgaaggtcggagtc-3′; reverse, 5′-gaagatggtgatgggatttc-3′; probe, 5′-VIC-caagcttcccgttctcagcc-TAMRA-3′. All real-time reverse transcription-PCR experiments were performed twice in duplicate in one 96-well plate. Using the comparative C_T method (PE Applied Biosystems), resulting C_t values were converted to picogram quantities according to each standard curve. HOXB13 and AR quantity was then normalized by GAPDH and subtracted from no reverse transcriptase controls. This value was then averaged for each duplicate.

Standard reverse transcription-PCR was performed to verify the expression of HOXB13, AR, prostate specific antigen, and β-actin in xenograft models. RNA from prostate tumor cell xenograft models was generously provided by Dr. Wytske M. van Weerden (Erasmus University, Rotterdam, The Netherlands). The primer sequences for each gene are as follows: HOXB13fw, 5′-ccccactgagtttgccttctatc-3′; HOXB13rv, 5′-gcctcttgtccttggtgatgaac-3′; ARfw, 5′-ggatgaggaacagcaaccttcac-3′; ARrv, 5′-atggacaccgacactgccttacac-3′; prostate specific antigen fw, gcagcattgaaccagaggag; prostate specific antigen rv, agaactggggaggcttgagtc; β-actinfw, 5′-gcaccacaccttctacaatgagc-3′; β-actinrv, 5′-tagcacagcctggatagcaacg-3′.

***In situ* Hybridization and Immunocytochemistry.** For *in situ* hybridization, a segment of human HOXB13 cDNA (350 bp) was amplified using a set of promoter sequence–linked primers in reverse transcription-PCR. The T7 promoter was incorporated into the HOXB13fw primer, and the SP6 promoter was incorporated into the HOXB13fw primer. Labeled riboprobes were synthesized by *in vitro* transcription of PCR-amplified cDNA using digoxigenin-RNA labeling kit, SP6-T7 (Roche Diagnostics, Indianapolis, IN) as described by the manufacturer. *In situ* hybridization was performed as described previously (20). For immunocytochemistry, human embryonic kidney 293 cells were plated onto two-well chamber slides, and pFLAG-HOXB13 was transfected. After 24 hours, cells were fixed and probed with anti-FLAG antibodies. Staining was developed using 3-amino, 9-ethyl-carbazole chromogen.

Transient Transfections. Approximately 1×10^5 cells were plated in a 24-well plate 16 hours before transfection. To see the hormone effect, cells were grown under 5% charcoal dextran–treated (CDT) FBS for 3 days before the transfection. Transfections were carried out using LipofectAMINE 2000 (Invitrogen) with 0.1 μg of reporter, 0.1 μg of test plasmid, and 20 ng of pCMV-βgal as described by the manufacturer's protocol. Six hours after transfection, the cells were washed and fed with medium containing 5% CDT-FBS. If needed, cells were treated with either R1881 synthetic androgen or ethanol. After 36 hours, cells were washed with PBS, lysed with 100 μL of passive lysis buffer, and assayed for luciferase activity as relative light units using Luciferase assay system (Promega). β-Galactosidase activity was assessed for the normalization and transfection efficiency. Lysates (15 μL) were incubated in 150 μL of ONPG solution (1 mmol/L $MgCl_2$, 0.8 mg/mL *o*-nitrophenyl-β-D-galactopyranoside, 0.1 mol/L sodium phosphate, and 45 μmol/L β-mercaptoethanol) at 37°C for 30 minutes. Reactions were stopped by the addition of 200 μL of 1 mol/L Na_2CO_3, and activity was measured as absorbance at 420 nm. Transfection experiments were done in triplicate and results are reported as mean ± *SD*.

Small Interfering RNA Transfection. For RNAi assay, small interfering RNA corresponding to the nucleotide positions 837 to 855 of human HOXB13 (relative to stop codon) were synthesized by Dharmacon (Lafayette, CO). The selected sequences (5′-gaacagcgcuaccccuuaa-3′) were submitted to BLAST searches against the nonredundant protein database in National Center for Biotechnology Information to make sure that only the selected genes were targeted. Lamin A/C SMARTpool Reagent (Dharmacon) was used as a nonspecific control. LNCaP cells were cultured onto 24-well plate in RPMI containing CDT-FBS for 2 days before the transfection. Transfections were carried out using DOTAP (Roche Diagnostics) with 0.1 μg of reporter, 5 to 25 nmol/L small interfering RNA, and 20 ng of pCMV-βgal. After 48 hours, reporter activity was measured as described above. For rescue assays, two silent nucleotide changes were introduced into the region complementary to HOXB13 small interfering RNA. The region gaacagcgc*tac*ccctta was mutated to gaacagcgc*caca*ccttaa, leaving the amino acid sequences unchanged. Mutations were accomplished by PCR using pFLAG-HOXB13 as a template. Primers used were 5′-aaggtgaagaacagcgccacacc-3′ and 5′-ggcgagaaccttct-tctctttg-3′. Amplified fragments were ligated with Rapid ligation kit (Roche Diagnostics). Sequencing analysis was done to verify the mutations.

Western Blotting Assay. Cells were grown up to 80% confluence in P60 culture dishes containing 5% FBS-T medium. Cells were then lysed in protein extraction buffer (1× Tris-buffered saline, 1% Nonidet P-40, 0.5% sodium deoxycholate, 0.1% SDS, and protease inhibitors) followed by needle sonication to break up the ribonucleosome. Twenty μg of total cell lysates were loaded onto 10% Bis-Tris gel (Invitrogen) and separated using the Novex electroporation system (Invitrogen). After proteins were transferred to polyvinylidene difluoride membrane, primary antibodies were applied, followed by incubation with horseradish peroxidase–conjugated secondary antibodies. Blots were developed by the ECL detection system (Pierce, Rockford, IL).

Coimmunoprecipitation Assay. LNCaP cells were grown under 5% CDT-FBS for 3 days and then infected with recombinant Ad-GFP-HOXB13 virus [5 multiplicity of infection (MOI)] and cultured in medium containing CDT-FBS. A 10 nmol/L final concentration of R1881 was added. Nuclear extracts were collected as described previously (21). Nuclear extracts (100 μg) were preincubated with 4 μg of AR-PG21 antibodies (Upstate Biotechnology) for 3 hours at 4°C, followed by adding protein A/G agarose (Santa Cruz Biotechnology).

To precipitate FLAG-HOXB13, nuclear extracts were directly mixed with EZView Red Anti-flag M2 Affinity Gel (Sigma). The mixture was incubated overnight at 4°C. Immunoprecipitates obtained by centrifugation were washed with Tris-buffered saline three times and eluted with 2× SDS loading buffer. Proteins were separated on 10% SDS-PAGE, and immunoblotting was followed by using either anti-AR antibodies (441; Santa Cruz Biotechnology) or anti-FLAG antibodies.

Growth Assays. Colony formation assay was performed as described previously (16). LNCaP cells were also monitored under the fluorescence microscope after virus infection to see the functional relation between HOXB13 and AR. In brief, LNCaP cells were infected with either Ad-GFP or Ad-GFP-HOXB13 at 2 MOI under the influence of androgen. For the coinfection study, LNCaP cells were grown under CDT-FBS for 3 days before the virus treatment. Recombinant AR virus (Ad-CMV-AR) was added to every well (1 MOI), together with either Ad-GFP or Ad-GFP-HOXB13 (1 MOI) as described above. At the same time, cells were treated with either R1881 (10 nmol/L) or ethanol. Infectivity and cell viability were carefully monitored by fluorescence microscopy for 10 days. Every 3 to 4 days, fresh medium was added. A 3-(4,5-dimethylthiazol-2-yl)-2,5-diphenyltetrazolium bromide (MTT) *in vitro* proliferation assay was also performed as described previously (16). In brief, cells were plated on a 24-well plates and infected with Ad-CMV-AR (2 MOI) and either Ad-GFP-HOXB13 or Ad-GFP (2 MOI) followed by the addition of 10 nmol/L R1881. At five days after virus infection, cells were stained with 100 μL of 5 mg/mL MTT solution and incubated for 2 hours at 37°C. The reaction was stopped by adding 400 μL of extraction buffer [50% formamide and 10% SDS (pH 4.7)]. After overnight incubation at 37°C, the absorbance at 570 nm was measured using a Spectra Microplate Reader (Molecular Devices, Sunnyvale, CA). Densitometric values were analyzed with Student's *t* test, using GraphPad Prism software (GraphPad, San Diego, CA).

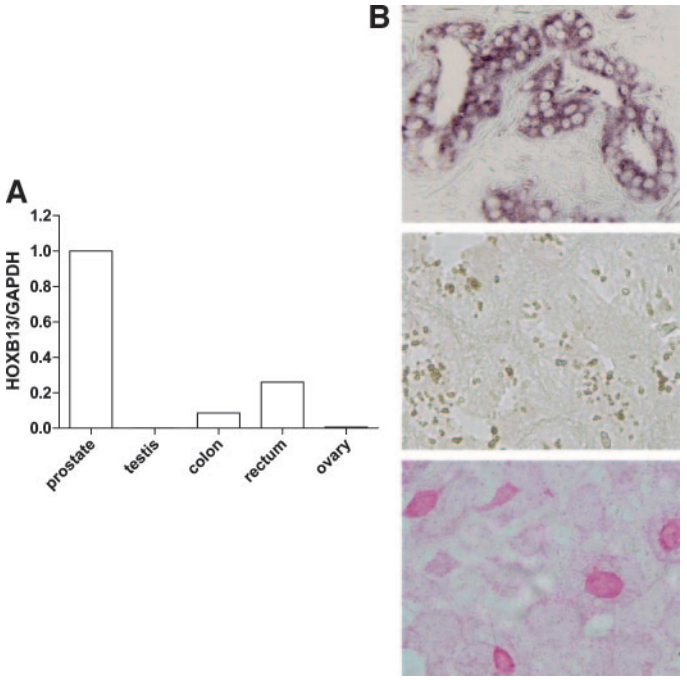

Fig. 1. Real time reverse transcription-PCR analysis of HOXB13 in normal human tissues. *A*. Real time reverse transcription-PCR combined with Taqman probe was performed with 50 ng of total RNA from various human normal tissues. RNA from the prostate was used as reference RNA and for drawing the standard curves for both HOXB13 and GAPDH. C_t values were converted to relative RNA concentration, which was normalized by GAPDH and further subtracted by no reverse transcriptase control. *Y*-axis numbers are relative values to the prostate, arbitrarily set as 1. Only tissues expressing HOXB13 are shown in this figure. *B*. *In situ* hybridization was performed to localize the expression of *HOXB13* RNA in prostate tumors (*top panel*; magnification, ×20). Sense strand was used as a negative control on serially cut section (*middle panel*; magnification, ×20). To identify the subcellular distribution of HOXB13, human embryonic kidney 293 cells were transfected with pFLAG-HOXB13 followed by immunocytochemical staining (*bottom panel*; magnification, ×40).

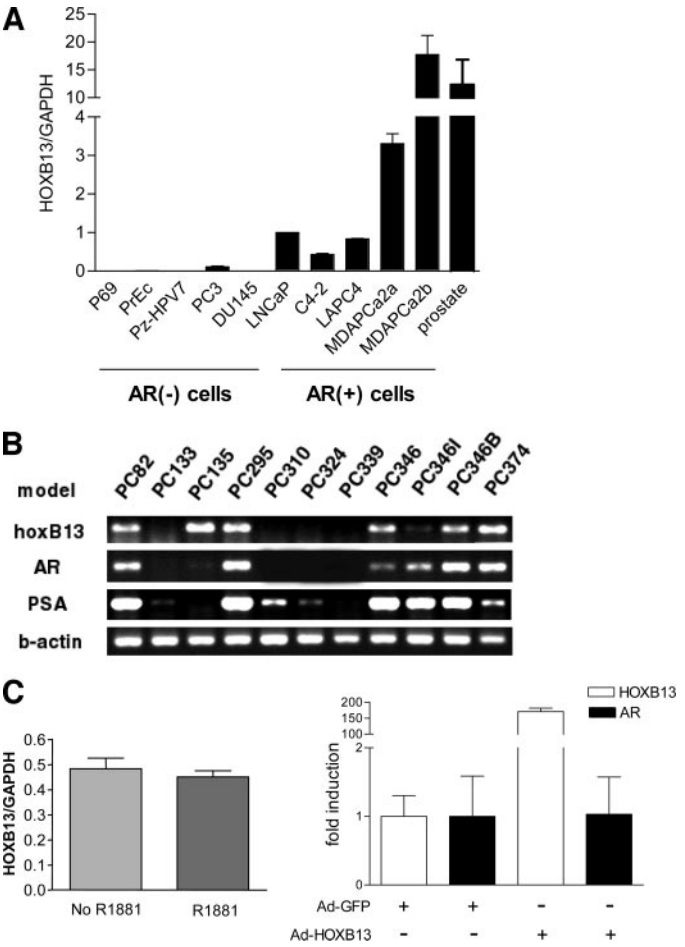

Fig. 2. Expression of HOXB13 is decreased in prostate cancer cells. *A*. Real time reverse transcription-PCR was performed as described in Fig. 1. Experiments were done in duplicate. The HOXB13 value from LNCaP was arbitrarily set as 1-fold. *B*. Regular reverse transcription-PCR was performed with RNAs from human tumor cell xenograft models. The level of HOXB13 from each cell was compared with the levels of AR and prostate specific antigen. *C*. To test whether one can induce the other between HOXB13 and AR, LNCaP cells were grown in CDT-FBS for 48 hours before the addition of either R1881 (*left panel*) or Ad-GFP-HOXB13 (*right panel*). After 48 hours, total RNA was extracted followed by real-time reverse transcription-PCR analysis as described in Fig. 1. Each *bar* represents the mean ± *SD*.

RESULTS

Expression of HOXB13 Is Specific to Prostate and Colorectum. Real-time reverse transcription-PCR was performed to determine the level of *HOXB13* mRNA expression in various normal human tissues. No functional antibodies are available at this point. Fig. 1*A* represents selective tissues that express substantial amounts of *HOXB13* mRNA. *HOXB13* was abundantly expressed in prostate (arbitrarily designated as 1-fold) and colorectal tissues (0.08–0.25-fold) compared with ovary and testis (≤0.005-fold). The other tissues tested (brain, cerebellum, spinal cord, lung, trachea, thymus, thyroid gland, heart, liver, mammary gland, pancreas, salivary gland, stomach, small intestine, adrenal gland, kidney, spleen, bone marrow, uterus, placenta, skin, and skeletal muscle) did not express a considerable amount of *HOXB13* mRNA, below 0.005-fold compared with the prostate (data not shown). In mouse Hoxb13 study, *Hoxb13* mRNA is confined to prostate, distal colon, and rectum (13). To localize *HOXB13* mRNA, *in situ* hybridization using *HOXB13* riboprobe was performed in prostate tumors. *HOXB13* RNA was exclusively localized to luminal epithelial cells of the prostate (Fig. 1*B*, *top panel*), whereas sense strand of *HOXB13* probe did not show signal (Fig. 1*B*, *middle panel*). There were mixed populations of *HOXB13*-positive and -negative cells among tumor samples (data not shown). In addition,

immunocytochemical staining of FLAG-HOXB13–transfected cells demonstrated that HOXB13 is predominantly localized at the nucleus (Fig. 1*B*, *bottom panel*).

Expression of HOXB13 Is Limited in AR-Positive Prostate Cancer Cells. The level of *HOXB13* was determined in prostate cells using real-time reverse transcription-PCR analysis. RNAs from normal prostate were used for comparison. To reduce sampling error, RNA for normal prostate was acquired from three different sources. As shown in Fig. 2*A*, *HOXB13* was limitedly expressed in all prostate cancer cells compared with normal prostate, except that *HOXB13* was highly expressed in MDA PCa 2b cells. MDA PCa 2b cells are developed from bone-metastasized androgen-independent tumors and have two mutations in ligand-binding site, and its growth is believed to be dependent on androgen-independent pathway (22–24). Interestingly, all prostate cancer cell lines retaining AR (AR positive) expressed moderate to high levels of *HOXB13* (LNCaP, C4–2, LAPC-4, and MDA PCa), whereas AR-negative cells had low to undetectable amounts of *HOXB13*. AR-negative cells include PC3 and DU145, most progressive (metastatic) and malignant cells, and immortalized normal prostate cells (P69, PrEc, and Pz-HPV7). Sequencing analysis showed that LNCaP and MDA PCa 2b cells did not retain any mutations in HOXB13 coding region. Using regular reverse transcription-PCR, prostate tumor cell xenograft models were evaluated for the expression of *HOXB13* and AR. These models are known to be more genetically stable than cultured cells, have a more homogeneous population than patient samples, and include both androgen-dependent and -independent cells (25, 26). This system provides valuable information because the *HOXB13* expression level was not altered in patient samples of prostate cancer compared with matching benign tissues due to the well-known heterogeneous population of prostate cancer (data not shown). Tumor cell xenograft models showed the same phenomenon of correlated expression pattern of *HOXB13* and AR (Fig. 2*B*). Only PC-135 showed a different expression pattern, a finding that needs to be further investigated. Then we tested whether *HOXB13* is controlled by androgen using the testosterone derivative R1881 in LNCaP cells. Cells (2×10^5) were plated in duplicate and grown for 48 hours with or without 10 nmol/L R1881. Total RNA was extracted and used for real-time reverse transcription-PCR analysis. As shown in Fig. 2*C* (*left panel*), the addition of R1881 did not significantly alter the level of *HOXB13* mRNA. This result is consistent with the mouse study (13). Conversely, overexpression of HOXB13 did not regulate the expression of AR RNA (Fig. 2*C*, *right panel*). These observations suggest that HOXB13 expression is regulated in androgen-independent manner, and its loss or decrease may be an important step for prostate tumor progression process.

HOXB13 Specifically Represses Hormone-Stimulated Androgen Receptor Transcriptional Activity. To determine whether there was any mechanistic and functional association between HOXB13 and AR, transient transfection combined with reporter transcription analysis was performed. First, we used the androgen response element core region of the prostate-specific antigen promoter linked to luciferase (pGL-AREc-luc). HOXB13 repressed about 50% of androgen-activated AR activity on this prostate specific antigen promoter, whereas HOXB13 did not inhibit hormone-independent AR activity (Fig. 3*A*). Then we used four copies of androgen response elements cloned into a pGL-TATA-luc vector (Promega), pGL-ARE4-luc. As shown in Fig. 3*B*, transfection of HOXB13 into AR-positive prostate cancer cells induced 3- to 4-fold suppression of androgen-activated AR transcriptional activity. Moreover, cotransfection of HOXB13 and AR into AR-negative cells caused greater inhibition activity (4–14-fold), notably more than a 10-fold decrease in PC3 prostate cancer cells (Fig. 3*C*). HOXB13-mediated inhibition of AR activity occurred in a dose-responsive manner (Fig. 3*D*) in LNCaP cells, and estradiol-

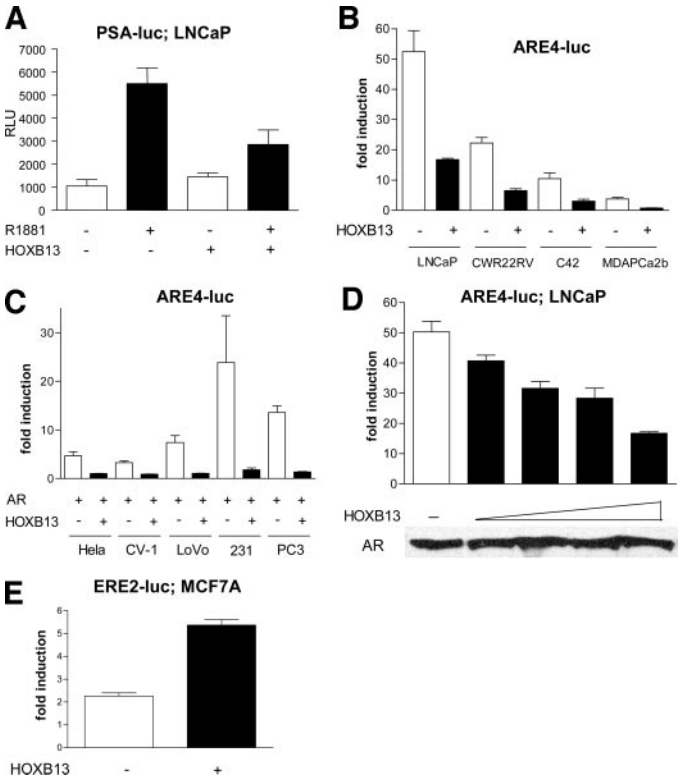

Fig. 3. HOXB13 suppresses hormone-activated AR signals. *A*. LNCaP cells were transiently transfected with 100 ng of pGL-prostate-specific antigen-Luc (*PSA-Luc*), 20 ng of pCMV-βgal, and 100 ng of pFLAG-HOXB13 with or without 10 nmol/L R1881. pFLAG-CMV was used as a counterpart of pFLAG-HOXB13. *B* through *D*, similar to *A* except that 4× androgen response element-luc (100 ng) was used. In *C*, pARO (25 ng) was cotransfected. In *D*, pFLAG-HOXB13 was used at different concentrations (25, 50, 100, and 200 ng). *E*. MCF7A cells were transfected with pGL-ERE2-luc under the control of estradiol. Luciferase assays were performed 48 hours post-transfection. Values indicate either relative luciferase unit (RLU) (luc/β-gal) or fold induction (RLU/basal activity without R1881). Each *bar* represents the mean ± *SD*.

stimulated estrogen receptor activity was not suppressed by HOXB13 in MCF7A cells (Fig. 3*E*). Previously, we demonstrated that HOXB13 promoted the transcriptional activity of the other universal promoters (16). These include SV40 and RSV promoters as well as general TATA, suggesting that HOXB13 may function as a general transcription factor in non-AR–mediated transactivation. To investigate whether forced expression of HOXB13 further down-regulates the expression of AR responsive genes, a HOXB13-expressing recombinant adenovirus (Ad-GFP-HOXB13) was used to overcome poor transfection efficiency in prostate cancer cells. This virus has shown high infectivity with minimal viral toxicity in a previous studies (16). LNCaP cells were infected with either Ad-GFP-HOXB13 or Ad-GFP viruses in the presence or absence of androgen for 36 hours followed by whole-cell lysate extraction and Western blot analysis. As shown in Fig. 4*A*, expression of androgen-activated prostate specific antigen was significantly decreased by the expression of HOXB13. Interestingly, overexpression of viral recombinant HOXB13 up-regulated the expression of AR protein without a known mechanism. To demonstrate whether the suppression of physiologic HOXB13 can promote the AR activity, we transfected HOXB13-specific small interfering RNA duplexes (Dharmacon) into LNCaP cells, in which HOXB13 is moderately expressed as shown in Fig. 2*A*. Transfection of HOXB13 small interfering RNA significantly increased hormone-stimulated AR activity in a dose-responsive manner (5–25 nmol/L final concentration), whereas a maximum dose of Lamin A/C small interfering RNA did not affect AR activity (Fig. 4*B*). To show the specificity of small interfering RNA, mutant form of pFLAG-HOXB13 vector

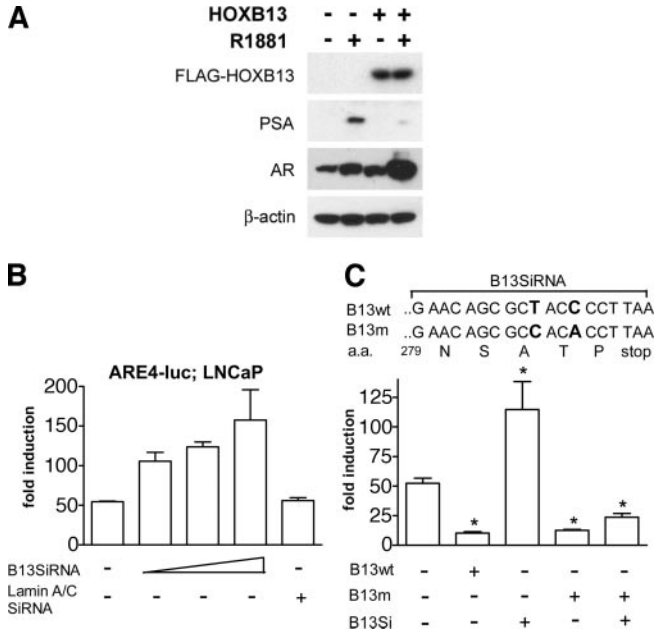

Fig. 4. Alterations of HOXB13 expression adequately modify hormone-activated AR signals. *A*. LNCaP cells were grown in 5% CDT-FBS for 72 hours before infection with either Ad-GFP-HOXB13 or Ad-GFP control virus (5 MOI). Cells were treated with R1881 (10 nmol/L) after virus infection. After 48 hours, whole-cell lysates were extracted, followed by Western blot analysis. *B*. LNCaP cells were transfected with final concentrations of 5 to 25 nmol/L HOXB13 small interfering RNA or 25 nmol/L Lamin A/C small interfering RNA, followed by luciferase assay. *C*. Mutated sequence is shown in the rescue plasmid, pFLAG-HOXB13m (*top panel*). Two silent mutations of nucleotide and amino acid (*a.a.*) sequences are indicated. *Bottom panel*, hormone-induced AR activity altered by the transfections of B13wt or B13m (100 ng) and/or B13 small interfering RNA (25 nmol/L) into LNCaP cells. pFLAG-CMV was used as a counterpart of either wild-type or mutant pFLAG-HOXB13. *, significant differences at each bar compared with no B13 constructs transfected ($P < 0.05$).

refractory to small interfering RNA was made by two silent third-base point mutations. As shown in Fig. 4*C*, cotransfection of mutant HOXB13 almost completely negated the activity of HOXB13 small interfering RNA in ARE4-luc system.

HOXB13 Physically Interacts with Androgen Receptor. To see whether there is any physical interaction between HOXB13 and AR and/or its accessory proteins, coimmunoprecipitation assay was performed. Nuclear extracts from LNCaP cells infected with Ad-GFP-HOXB13 were immunoprecipitated with either anti-Flag antibodies or AR-specific antibodies followed by Western blot analysis. As shown in Fig. 5, either Flag-HOXB13 or AR was detected by its counterpart antibodies, whereas no band was detected with normal immunoglobulin G control. However, HOXB13 does not possess the LXXLL or FXXLF motif, common motifs in AR-interacting proteins. These results suggest that HOXB13-mediated suppression of AR activity is accomplished through interacting with AR.

Androgen Receptor Activity Suppressed by HOXB13 Can Be Restored by Overexpression of Coactivators and Androgen Receptor. To investigate whether HOXB13 can inhibit the synergistic function of p160 coactivators, knowing that HOXB13 binds to AR, LNCaP cells were cotransfected with AIB-1 or TIF-2 with pGL-ARE4-luc followed by reporter gene transcription assay as described above. Although HOXB13 significantly suppressed androgen-activated AR activity, synergistic activity induced by overexpression of either AIB-1 or TIF-2 was not completely abolished (Fig. 6*A*). This result suggests that HOXB13 may affect AR-mediated transcriptional activity without disturbing the coactivator function of p160 coactivators. We then tested whether the suppressive function of HOXB13 can be rescued by the overexpression of AR. CV-1 monkey kidney cells were cotransfected with HOXB13 and an increased amount of AR (Fig. 6*B*). The addition of AR partially restores the transcriptional activity of AR, suggesting that HOXB13 and AR may functionally counteract to manifest coactivator-mediated transcriptional activity.

Androgen-Activated Androgen Receptor Counteracts HOXB13-Mediated Growth Suppression. To observe the growth-modulating function of HOXB13, a colony formation study combined with the transfection of HOXB13 was performed. HOXB13 expression vector (pIRES-HOXB13) was transfected into three different p60 dishes of LNCaP cells, followed by the selection of transfected cells in neomycin-containing medium. pIRES-neo vector was used as a control. Two weeks later, the numbers of surviving clones were observed under the microscope and counted. As shown in Fig. 7*A*, overexpression of HOXB13 dramatically inhibited cell growth (9.7 ± 1.3 colonies) compared with controls (0.3 ± 0.3 colonies). In addition, HOXB13 seems to drive LNCaP cells into terminal differentiation status, characterized by large nuclei and cytoplasm. Additional analysis using

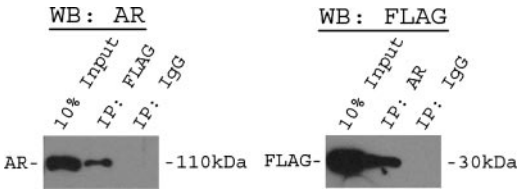

Fig. 5. HOXB13-mediated AR suppression is due to interaction with AR. For the *in vivo* interaction of HOXB13 and AR, coimmunoprecipitation was performed. LNCaP cells were infected with Ad-GFP-fHOXB13 virus in the presence of androgen, and nuclear extracts were collected 48 hours after infection. One hundred μg of proteins were mixed with 4 μg of either anti-AR antibodies (Upstate Biotechnology; PG21) or anti-FLAG antibodies, followed by conjugation to agarose A/G beads. Normal immunoglobulin G (*IgG*) was used as negative control. Precipitated fractions (*IP*) were resolved by SDS-PAGE and analyzed by Western blot (*WB*) using either anti-FLAG antibodies or anti-AR antibodies.

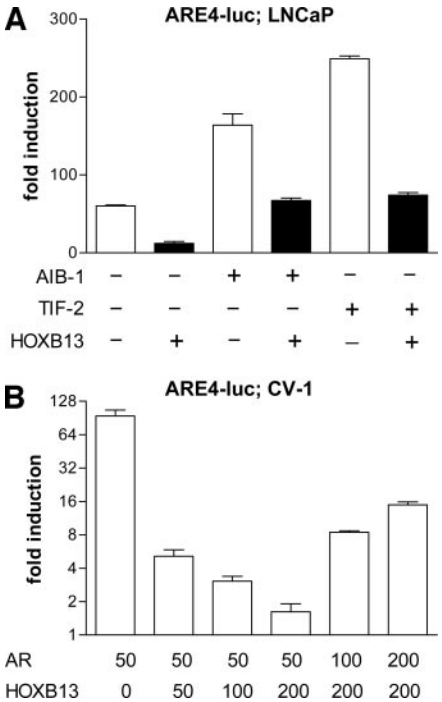

Fig. 6. AR partly restores the activity suppressed by HOXB13. *A,* LNCaP cells were cotransfected with pGL-ARE4-luc (100 ng), pAd1020-AIB1 or pAd1020-TIF2 (100 ng), and pFLAG-HOXB13 (100 ng) under the control of R1881. Control vectors (pFLAG-CMV and pAd1020) were used to match coactivator DNA. Relative luciferase activity was measured, and the hormone-treated group was normalized by the non-hormone–treated group. Values were represented as fold induction. *B*, CV-1 cells were cotransfected with pGL-ARE4-luc, pFLAG-HOXB13, and pARO as indicated. Each *bar* represents the mean ± *SD*.

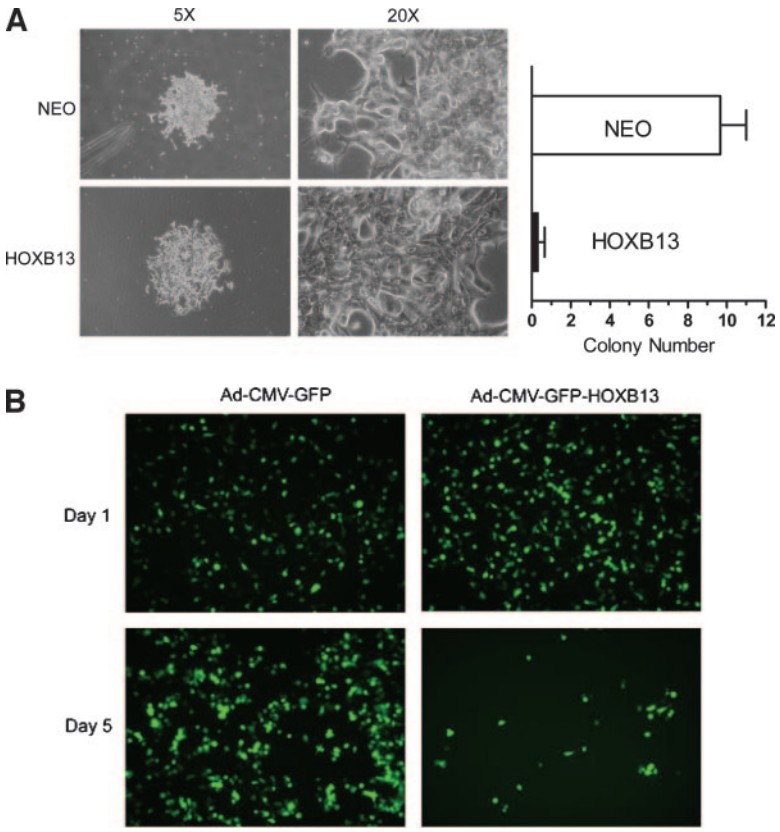

Fig. 7. HOXB13 suppresses the growth of LNCaP cells. *A*. LNCaP cells were transfected with either pIRES-HOXB13 or pIRES-neo vectors in triplicate followed by neomycin (G418; 400 μg/mL) selection. After 2 weeks, isolated colonies were counted. Each *bar* represents the mean $\pm$ *SD*. *B*, LNCaP cells in the presence of androgen were infected with either Ad-GFP-HOXB13 or Ad-GFP virus (2 MOI). Then GFP-expressing cells were monitored under the fluorescence microscope.

viral recombinant HOXB13 demonstrated that HOXB13 significantly decreased the number of GFP-expressing cells at 5 days after virus infection (Fig. 7*B*). This result suggests that HOXB13 functions as a negative growth regulator of AR-expressing LNCaP cells.

To confirm whether the growth-suppressive function of HOXB13 is mediated by affecting the androgen-AR signal, AR was overexpressed via adenoviral vector in LNCaP cells in the presence of androgen. As demonstrated in Fig. 8*A*, cells were infected with Ad-CMV-AR virus (1 MOI) combined with either Ad-GFP-HOXB13 or Ad-GFP virus (1 MOI). Cells were closely monitored under the fluorescence microscope. At day 1 after infection, most cells expressed GFP, and each group showed a similar number of GFP-expressing cells. At day 10, HOXB13-mediated growth suppression was significantly retarded by the addition of androgen-activated AR. To confirm the result that overexpression of AR can rescue HOXB13-mediated growth suppression under the influence of androgen, an *in vitro* MTT proliferation assay was performed after the cells (LNCaP and CV-1) were infected with a combination of Ad-CMV-AR and either Ad-GFP-HOXB13 or Ad-GFP virus (2 MOI for each virus). At a final concentration of 10 nmol/L, R1181 was added to all of the cells immediately after virus infection. At 5 days after virus infection, cells were stained with MTT and the O.D. was measured. As shown in Fig. 8*B*, HOXB13 suppressed the growth of both LNCaP and CV-1 cells compared with the Ad-GFP–infected group. Growth-suppressive effect by HOXB13 was higher in CV-1 cells than in LNCaP cells, suggesting that endogenous AR may exert growth protection in LNCaP cells. Meanwhile, infection with AR virus also suppressed the growth of both LNCaP and CV-1 cells in the presence of hormone. AR is well known to have a biphasic effect depending on the activation status of AR, and overactivation of AR drives cells into an apoptotic process and cell death (27–29). However, coinfection of AR virus in the presence of androgen counteracts the growth-suppressive effect of HOXB13 in LNCaP cells, but not in CV-1 cells. This suggests that HOXB13 and AR functionally counteract each other in AR-intact cells and that balance between these two proteins is important for cells to avoid abnormal proliferation. Previously, we have demonstrated that HOXB13 suppresses the growth of AR-negative cells, including CV-1, by affecting the β-catenin/TCF signaling pathway (16). Therefore, overexpression of AR in androgen-insensitive CV-1 cells did not affect the growth-suppressive function of HOXB13, which may be accomplished by affecting β-catenin/TCF signaling rather than androgen-AR signaling.

DISCUSSION

An immense effort has been made to understand the regulation of complex androgen-AR signals. Nuclear receptor cofactors are believed to have a central role in this essential growth-regulating pathway. Although more than 100 coactivators are reported to stimulate steroid receptors, limited numbers of corepressors are known to confer negative signals for this pathway. The best-known corepressors are NCoR/SMRT, which are constitutive transcriptional repressors and bind to their cognate DNA-binding sites in the absence of ligand. Although the repressive function of NCoR/SMRT has been reported in some ligand-activated steroid receptors (30, 31), the mechanistic role of these universal nuclear receptor corepressors is not well understood in the regulation of steroid receptor–mediated activity, including AR. Recently, cyclin D1 and ARA67/PAT1 have been shown to function as AR repressors, mainly by interacting with the NH_2-terminal region of AR (32, 33). The NH_2-terminal enhancer of split (AES) is also known to repress AR activity (34). Our data demonstrate that HOXB13 functions as a novel repressor for androgen-activated AR transcriptional activity and subsequently modulates the positive growth signal stimulated by AR. Expression of HOXB13 was highly specific to the prostate and HOXB13 did not suppress hormone-activated estrogen receptor transcriptional activity, suggesting that HOXB13 may function as an AR-specific repressor. Using cultured prostate cancer cells and xenograft models, we have also demonstrated that expression of

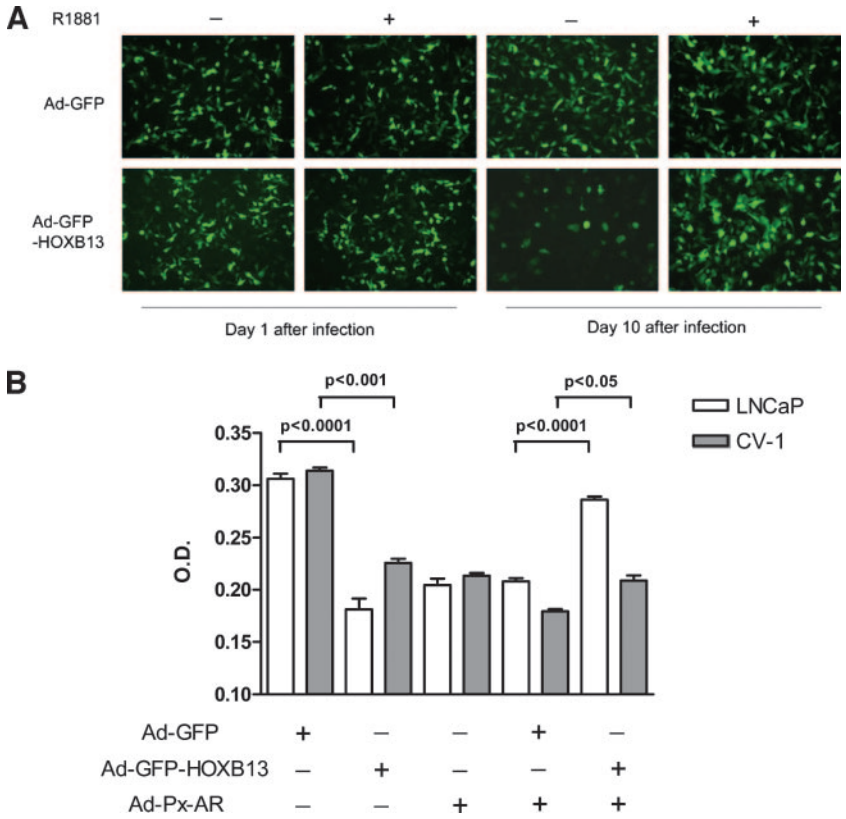

Fig. 8. AR counteracts the function of HOXB13. *A*. LNCaP cells were infected with Ad-CMV-AR virus along with either Ad-GFP-HOXB13 or Ad-GFP viruses with or without R1881. GFP-expressing cells were monitored under the fluorescence microscope. *B*. The same study was performed as in *A*. Both LNCaP and CV-1 cells were treated with either R1881 or ethanol after virus infection. Five days later, cells were stained with MTT reagent, and absorbance at 570 nm was measured. Only R1881-treated cells are shown. The *P* values in the diagram, determined by two-tailed Student's *t* test, correspond to the difference between two groups.

HOXB13 is restricted to AR-expressing prostate cells and is not controlled by androgen. Altogether, HOXB13 may be a very important negative regulator of androgen-activated AR transactivation, which can modulate the suppression of androgen-AR–mediated growth stimulation.

Hox proteins are known to play pivotal roles in maintaining homeostasis in normal cell proliferation and differentiation. Despite intensive research, the mechanism of action of Hox proteins remains unclear. A paradigm that the Hox proteins function as transcription factors was set, merely due to the presence of the DNA-binding homeodomain (35). However, large numbers of Hox proteins alone do not bind to target DNA with high affinity or specificity (36), but require other homeodomain proteins to form cooperative DNA-binding complexes, such as Pbx/Exd and Meis/Prep/Htx (37). Pbx proteins physically interact with the YPWM motif of the Hox proteins, but Hoxb13 does not have a typical YPWM motif and consequently does not interact with Pbx/Exd. A few studies have reported the involvement of Hox proteins in nuclear receptor regulation. For example, Hoxa5 transactivates the progesterone receptor promoter (38). On the other hand, Hox proteins are also involved in the regulation of coactivator function without DNA binding. Shen *et al.* (39) reported that most Hox proteins, including the Hox-13 paralog, bind to CBP/p300 coactivators through their homeodomain. CBP/p300 does not form DNA-binding complexes with the Hox proteins, but instead prevents their binding to DNA, suppressing the transactivating function of Hox protein. Conversely, Hox proteins inhibit the activity of CBP, suggesting that Hox proteins may inhibit CBP histone acetyltransferase activity and thus function as repressors of gene transcription. In our study, the AR-suppressive function of HOXB13 was mediated through the interaction with AR although its association with androgen response element remains to be seen, suggesting that HOXB13 may have a transcription-regulating function as a nontranscription factor. To understand the mechanism on HOXB13-mediated suppression of AR activity, communication between HOXB13 and CBP/p300 needs to be clarified.

Recently, we demonstrated that HOXB13 functions as a growth suppressor of AR(−) and HOXB13(−) PC3 cells by the negative regulation of the β-catenin/TCF-4 signal, specifically down-regulating the expression of TCF-4 transcription factor (16). As demonstrated by others (40, 41), we have observed that LNCaP cells did not respond well to β-catenin/TCF-4 signaling due to the low level of TCF-4 expression, suggesting that HOXB13-mediated growth suppression in LNCaP does not result from the suppression of β-catenin/TCF-4 signaling as we observed in PC3 cells. Both androgens and TCF-4 are highly expressed in prostate cancer and generally known to cause increased proliferation of prostate cancer cells (42, 43). Therefore, the growth-suppressive function of HOXB13 is thought to be accomplished through two different growth-modulating pathways, depending on the status of endogenous AR. Although there is increased evidence on the potential communication between AR and β-catenin/TCF signaling, such as the physical interaction of AR with β-catenin (44) or TCF-4 (40), there is little possibility that HOXB13 functions as a mediator to control these two important signaling pathways for the following reasons: (1) AR transactivation is suppressed by overexpression of TCF-4 (activation of β-catenin; refs. 40 and 44), which HOXB13 negatively controls, and (2) HOXB13 physically interacted with neither β-catenin nor TCF-4 (data not shown). It is also possible that HOXB13 may use both signaling pathways to suppress the growth of AR-positive cells. Androgen-independent CWR22RV cells express moderate levels of AR and consequently manifest AR activity and β-catenin/TCF signaling activity and TCF-4 expression (40, 41). We have observed that HOXB13 regulates both signaling pathways in CWR22RV cells by reporter transcription assay (Fig. 3*B*; ref. 16). Therefore, the loss of AR or inactivation of AR signaling may result in more involvement of HOXB13 in the regulation of β-catenin/TCF signaling, such that cancer cells need to lose HOXB13 expression to acquire a growth advantage. This assumption suggests that the loss of HOXB13 may be an important step in the survival mechanism of androgen-independent prostate cancer cells. At the same time, AR counteracts the

suppressor function of HOXB13, so that HOXB13 and AR need to coexist for prostate cancer cells to survive.

ACKNOWLEDGMENTS

We are grateful to Dr. Chinghai Kao for critical discussions and advice and to Juan Antonio Jimenez for scientific editing. We also thank Drs. Jer-Tsong Hsieh and Wytske M. van Weerden for providing RNA from cultured prostate cancer cells and xenograft models, respectively.

REFERENCES

1. Heinlein CA, Chang C. Androgen receptor (AR) coregulators: an overview. Endocr Rev 2002;23:175–200.
2. Onate SA, Boonyaratanakornkit V, Spencer TE, et al. The steroid receptor coactivator-1 contains multiple receptor interacting and activation domains that cooperatively enhance the activation function 1 (AF1) and AF2 domains of steroid receptors J Biol Chem 1998;273:12101–8.
3. Ma H, Hong H, Huang SM, et al. Multiple signal input and output domains of the 160-kilodalton nuclear receptor coactivator proteins. Mol Cell Biol 1999;19:6164–73.
4. Webb P, Nguyen P, Shinsako J, et al. Estrogen receptor activation function 1 works by binding p160 coactivator proteins. Mol Endocrinol 1998;12:1605–18.
5. Cheng S, Brzostek S, Lee SR, Hollenberg AN, Balk SP. Inhibition of the dihydrotestosterone-activated androgen receptor by nuclear receptor corepressor. Mol Endocrinol 2002;16:1492–501.
6. Cillo C, Cantile M, Faiella A, Boncinelli E. Homeobox genes in normal and malignant cells. J Cell Physiol 2001;188:161–9.
7. Takahashi Y, Hamada J, Murakawa K, et al. Expression profiles of 39 HOX genes in normal human adult organs and anaplastic thyroid cancer cell lines by quantitative real-time RT-PCR system. Exp Cell Res 2004;293:144–53.
8. Podlasek CA, Clemens JQ, Bushman W. Hoxa-13 gene mutation results in abnormal seminal vesicle and prostate development. J Urol 1999;161:1655–61.
9. Prins GS, Birch L, Habermann H, et al. Influence of neonatal estrogens on rat prostate development. Reprod Fertil Dev 2001;13:241–52.
10. Podlasek CA, Duboule D, Bushman W. Male accessory sex organ morphogenesis is altered by loss of function of Hoxd-13. Dev Dyn 1997;208:454–65.
11. Warot X, Fromental-Ramain C, Fraulob V, Chambon P, Dolle P. Gene dosage-dependent effects of the Hoxa-13 and Hoxd-13 mutations on morphogenesis of the terminal parts of the digestive and urogenital tracts. Development 1997;124:4781–91.
12. Zeltser L, Desplan C, Heintz N. Hoxb-13: a new Hox gene in a distant region of the HOXB cluster maintains colinearity. Development 1996;122:2475–84.
13. Sreenath T, Orosz A, Fujita K, Bieberich CJ. Androgen-independent expression of hoxb-13 in the mouse prostate. Prostate 1999;41:203–7.
14. Economides KD, Zeltser L, Capecchi MR. Hoxb13 mutations cause overgrowth of caudal spinal cord and tail vertebrae. Dev Biol 2003;256:317–30.
15. Economides KD, Capecchi MR. Hoxb13 is required for normal differentiation and secretory function of the ventral prostate. Development 2003;130:2061–9.
16. Jung C, Kim RS, Lee SJ, Wang C, Jeng MH. HOXB13 homeodomain protein suppresses the growth of prostate cancer cells by the negative regulation of T-cell factor 4. Cancer Res 2004;64:3046–51.
17. Lee SJ, Kim HS, Yu R, et al. Novel prostate-specific promoter derived from PSA and PSMA enhancers. Mol Ther 2002;6:415–21.
18. Cleutjens KB, van der Korput HA, van Eekelen CC, et al. An androgen response element in a far upstream enhancer region is essential for high, androgen-regulated activity of the prostate-specific antigen promoter. Mol Endocrinol 1997;11:148–61.
19. Wu TT, Sikes RA, Cui Q, et al. Establishing human prostate cancer cell xenografts in bone: induction of osteoblastic reaction by prostate-specific antigen-producing tumors in athymic and SCID/bg mice using LNCaP and lineage-derived metastatic sublines. Int J Cancer 1998;77:887–94.
20. Jung C, Ou YC, Yeung F, Frierson HF Jr, Kao C. Osteocalcin is incompletely spliced in non-osseous tissues Gene 2001;271:143–50.
21. Lee SJ, Lee K, Yang X, et al. NFATc1 with AP-3 site binding specificity mediates gene expression of prostate-specific-membrane-antigen. J Mol Biol 2003;330:749–60.
22. Navone NM, Olive M, Ozen M, et al. Establishment of two human prostate cancer cell lines derived from a single bone metastasis. Clin Cancer Res 1997;3:2493–500.
23. Navone NM, Rodriquez-Vargas MC, Benedict WF, et al. TabBO: a model reflecting common molecular features of androgen-independent prostate cancer. Clin Cancer Res 2000;6:1190–7.
24. Zhao XY, Peehl DM, Navone NM, Feldman D. 1 alpha,25-Dihydroxyvitamin D3 inhibits prostate cancer cell growth by androgen-dependent and androgen-independent mechanisms. Endocrinology 2000;141:2548–56.
25. Jongsma J, Oomen MH, Noordzij MA, et al. Different profiles of neuroendocrine cell differentiation evolve in the PC-310 human prostate cancer model during long-term androgen deprivation. Prostate 2002;50:203–15.
26. van Weerden WM, de Ridder CM, Verdaasdonk CL, et al. Development of seven new human prostate tumor xenograft models and their histopathological characterization. Am J Pathol 1996;149:1055–62.
27. Kokontis J, Takakura K, Hay N, Liao S. Increased androgen receptor activity and altered c-myc expression in prostate cancer cells after long-term androgen deprivation. Cancer Res 1994;54:1566–73.
28. Heisler LE, Evangelou A, Lew AM, Trachtenberg J, Elsholtz HP, Brown TJ. Androgen-dependent cell cycle arrest and apoptotic death in PC-3 prostatic cell cultures expressing a full-length human androgen receptor. Mol Cell Endocrinol 1997;126:59–73.
29. Brass AL, Barnard J, Patai BL, Salvi D, Rukstalis DB. Androgen up-regulates epidermal growth factor receptor expression and binding affinity in PC3 cell lines expressing the human androgen receptor. Cancer Res 1995;55:3197–3203.
30. Jackson TA, Richer JK, Bain DL, Takimoto GS, Tung L, Horwitz KB. The partial agonist activity of antagonist-occupied steroid receptors is controlled by a novel hinge domain-binding coactivator L7/SPA and the corepressors N-CoR or SMRT. Mol Endocrinol 1997;11:693–705.
31. Wagner BL, Norris JD, Knotts TA, Weigel NL, McDonnell DP. The nuclear corepressors NCoR and SMRT are key regulators of both ligand- and 8-bromo-cyclic AMP-dependent transcriptional activity of the human progesterone receptor. Mol Cell Biol 1998;18:1369–78.
32. Petre CE, Wetherill YB, Danielsen M, Knudsen KE. Cyclin D1: mechanism and consequence of androgen receptor co-repressor activity. J Biol Chem 2002;277:2207–15.
33. Zhang Y, Yang Y, Yeh S, Chang C. ARA67/PAT1 functions as a repressor to suppress androgen receptor transactivation. Mol Cell Biol 2004;24:1044–57.
34. Yu X, Li P, Roeder RG, Wang Z. Inhibition of androgen receptor-mediated transcription by amino-terminal enhancer of split. Mol Cell Biol 2001;21:4614–25.
35. Levine M, Hoey T. Homeobox proteins as sequence-specific transcription factors. Cell 1988;55:537–40.
36. Shen WF, Chang CP, Rozenfeld S, et al. Hox homeodomain proteins exhibit selective complex stabilities with Pbx and DNA. Nucleic Acids Res 1996;24:898–906.
37. Mann RS, Chan SK. Extra specificity from extradenticle: the partnership between HOX and PBX/EXD homeodomain proteins. Trends Genet 1996;12:258–62.
38. Raman V, Tamori A, Vali M, Zeller K, Korz D, Sukumar S. HOXA5 regulates expression of the progesterone receptor. J Biol Chem 2000;275:26551–5.
39. Shen WF, Krishnan K, Lawrence HJ, Largman C. The HOX homeodomain proteins block CBP histone acetyltransferase activity. Mol Cell Biol 2001;21:7509–22.
40. Amir AL, Barua M, McKnight NC, Cheng S, Yuan X, Balk SP. A direct beta-catenin-independent interaction between androgen receptor and T cell factor 4. J Biol Chem 2003;278:30828–34.
41. Chesire DR, Isaacs WB. Ligand-dependent inhibition of beta-catenin/TCF signaling by androgen receptor. T cell factor. Oncogene 2002;21:8453–69.
42. Denmeade SR, Lin XS, Isaacs JT. Role of programmed (apoptotic) cell death during the progression and therapy for prostate cancer. Prostate 1996;28:251–65.
43. Davies P, Eaton CL. Regulation of prostate growth. J Endocrinol 1991;131:5–17.
44. Song LN, Herrell R, Byers S, Shah S, Wilson EM, Gelmann EP. Beta-catenin binds to the activation function 2 region of the androgen receptor and modulates the effects of the N-terminal domain and TIF2 on ligand-dependent transcription. Mol Cell Biol 2003;23:1674–87.

HOXB13 Induces Growth Suppression of Prostate Cancer Cells as a Repressor of Hormone-Activated Androgen Receptor Signaling

Chaeyong Jung, Ran-Sook Kim, Hong-Ji Zhang, et al.

Cancer Res 2004;64:9185-9192.